metals

MDPI

Review

Low and Medium Carbon Advanced High-Strength Forging Steels for Automotive Applications

Koh-ichi Sugimoto [1,*], Tomohiko Hojo [2] and Ashok Kumar Srivastava [3]

[1] Department of Mechanical Systems Engineering, School of Science and Technology, Shinshu University, Nagano 380-8553, Japan
[2] Institute for Materials Research, Tohoku University, Sendai 980-8577, Japan; hojo@imr.tohoku.ac.jp
[3] Department of Metallurgical Engineering, School of Engineering, OP Jindal University, Raigarh 496109, India; ashok.srivastava@opju.ac.in
* Correspondence: sugimot@shinshu-u.ac.jp; Tel.: +81-90-9667-4482

Received: 28 October 2019; Accepted: 21 November 2019; Published: 26 November 2019

Abstract: This paper presents the microstructural and mechanical properties of low and medium carbon advanced high-strength forging steels developed based on the third generation advanced high-strength sheet steels, in conjunction with those of conventional high-strength forging steels. Hot-forging followed by an isothermal transformation process considerably improved the mechanical properties of the forging steels. The improvement mechanisms of the mechanical properties were summarized by relating to the matrix structure, the strain-induced transformation of metastable retained austenite, and/or a mixture of martensite and austenite.

Keywords: advanced high-strength forging steel; hot-forging; microstructure; retained austenite characteristics; mechanical properties; applications

1. Introduction

Conventional high-strength forging steels (CFSs) are necessary for the production of automotive powertrain and chassis parts. Most of the CFSs are generally subjected to the heat-treatment of quenching and tempering (Q&T) after cold- or hot-forging to increase the yield stress, impact toughness, fatigue strength, etc. Because the Q&T treatment is expensive, modified V-microalloying precipitation hardening ferritic/pearlitic (PHFP-M) steels and bainitic steels subjected to hot-forging and then controlling cooling were developed to eliminate the additional Q&T treatment [1–4]. Although both the steels are applied to the automotive powertrain and chassis forging parts, their mechanical properties are inferior to those of Q&T steels. Recently, non-heat-treated forging steels with further high mechanical properties are required to achieve the weight reduction and size-down of the automotive parts [3,4].

In the past decades, the following first, second, and third generation advanced high-strength steel (AHSS) sheets shown in Figure 1 have been developed for the weight reduction and the improvement of crush safety of the automotive body.

(I) First generation AHSS: ferrite–martensite dual-phase steels, transformation-induced plasticity (TRIP)-aided steels [5] with polygonal ferrite matrix structure, and complex phase steels [6–8].
(II) Second generation AHSS: twinning-induced plasticity (TWIP) high Mn steels [7–10].
(III) Third generation AHSS: TRIP-aided steels with bainitic ferrite, bainitic ferrite–martensite, and martensite matrix structures (TBF, TBM, and TM steels, respectively) [11–16], quench and partitioning (Q&P) steels [7,8,17–19], nanostructured bainitic (Nano-B) steels (or carbide free bainitic steels) [3,4,7,8,20–23], dual-phase type and martensite type medium Mn (M-Mn) steels [7,8,24–26], and maraging-TRIP steels [7,27].

The third generation AHSS sheets are the most needed steel sheet grade in the future by the automotive industry. In the third generation AHSS sheets, a product or combination of tensile strength and total elongation higher than 30 GPa% is made the target (Figure 1). Low and medium carbon TBF [8,11,12], TBM [11–15], and TM steels [12–16] are produced by a similar heat-treatment process to low and medium carbon Q&P, Nano-B, and martensite type M-Mn steels, except Q&P steel subjected to a two-step Q&P process. For the TBF, TBM, and TM steels, isothermal transformation (IT) processes at temperature (T_{IT}) above the martensite-start temperature (M_S) [11,12], between M_S and the martensite-finish temperature (M_f) [11–15] and lower than M_f are conducted after austenitizing or annealing [12–16], respectively. Recently, low and medium carbon TBF [28–30] and Q&P steels [31] were applied to the automotive body and seats because their steels possess a superior combination of tensile strength and cold formability.

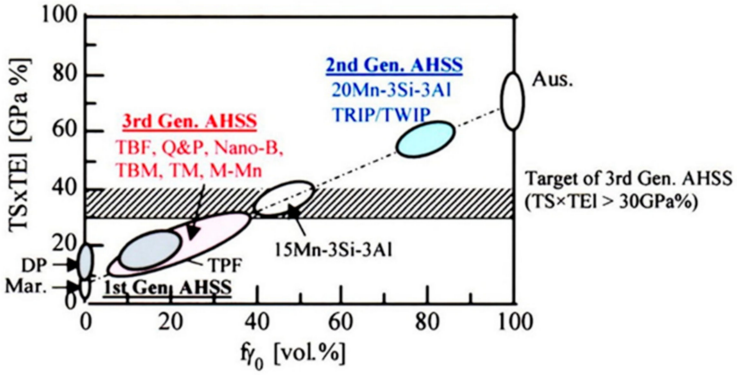

Figure 1. Relationship between the product of tensile strength and total elongation (TS × TEl) and initial volume fraction of austenite or retained austenite ($f\gamma_0$) in the first, second, and third generation advanced high-strength steel (AHSS) sheets. Mar.: conventional martensitic steel, DP: ferrite–martensite dual-phase steel, TPF, TBF, TBM, and TM: transformation-induced plasticity (TRIP)-aided steels with polygonal ferrite, bainitic ferrite, bainitic ferrite–martensite, and martensite matrix, respectively, Q&P: one-step and two-step quenching and partitioning steel, Nano-B: nanostructured bainitic steel, M-Mn: dual-phase type and martensite type medium Mn steel, TWIP: twinning-induced plasticity steel, Aus.: austenitic steel. This figure was modified based on Ref. [24].

The advanced high-strength forging steels (AFSs) which were developed based on the third generation AHSSs are also very attractive to apply to the automotive hot-forging parts because they bring on the especially high yield stress and tensile strength, large elongations and high impact toughness, high fatigue strength and high delayed fracture strength [32–37]. It is well known that the improved mechanical properties are associated with refined microstructure and improved retained austenite characteristics [32–36].

This paper introduces the microstructural and mechanical properties of the prospective low and medium carbon AFSs with bainitic ferrite and/or martensite matrix structure and metastable retained austenite, along with the low and medium carbon CFSs. In addition, the improvement mechanisms of the mechanical properties are detailed by relating to the matrix structure, the strain-induced transformation of metastable retained austenite and/or a mixture of martensite and austenite (MA). Unfortunately, this paper does not include various properties of dual-phase type M-Mn [24,25] and maraging-TRIP steels [27], because heat-treatment process and chemical composition of both the steels are great different from those of the other AFSs.

2. Classification of Hot-Forging Process for Low and Medium Carbon Steels

The hot-forging process of various low and medium carbon forging steels is classified as Table 1. The forging process can be divided into three categories such as conventional hot-forging, controlled hot-forging (or semi-hot-forging), and ausforming. Conventional hot-forging temperatures

are between 1000 °C and 1200 °C above the recrystallized temperature (T_R). Controlled forging temperatures are between T_R and Ac_3. Ausforming temperatures are lower than Ac_3 corresponding to a metastable austenite region. The lower the forging temperature, the finer the microstructure. For every forging, post cooling rates decide the type of matrix structure, namely, quenching, rapid cooling, and moderate cooling resulting in martensite, bainite, and ferrite-pearlite matrix structures, respectively. Microalloying of V, Ti, and/or Nb contributes to the refining of prior austenitic grain and the precipitation strengthening of the matrix structure by V,Ti,Nb(C,N)-carbonitrides [8,38–45]. Microalloying of Cr, Mo, Ni, B, etc. increases the hardenability and resultantly enhances the yield stress and tensile strength of the forging products.

Table 1. Classification of hot-forging process for low and medium carbon steels. PHFP steel: V-microalloying precipitation hardening ferritic-pearlitic steel, PHFP-M steel: modified PHFP steel, Q&T steel: quenching and tempering steel, TBF steel: TRIP-aided bainitic ferrite steel, Q&P steel: quenching and partitioning steel, Nano-B steel: nanostructured bainitic steel, TBM steel: TRIP-aided bainitic ferrite-martensitic steel, TM steel: TRIP-aided martensitic steel, M-Mn steel: medium Mn steel, T_R: recrystallized temperature.

Designation	Forging Temperature	Phase on Forging	Steel Type after Hot-Forging		
			Diffusion Transformation	Non-Diffusion and Diffusion Transformation	Non-Diffusion Transformation
Conventional hot-forging	$>T_R$	austenite	PHFP steel, PHFP-M steel, bainitic steel, TBF steel, one-step Q&P steel, Nano-B steel	Two-step Q&P steel, TBM steel	Q&T steel, TM steel, Martensite type M-Mn steel
Controlled hot-forging	$T_R - Ac_3$	austenite			
Ausforming	$<Ac_3$	metastable austenite			

3. Conventional High-Strength Forging Steels; CFSs

Figure 2 shows the typical hot-forging and subsequent controlling cooling diagrams of the CFSs such as Q&T, PHFP-M, and bainitic steels [46]. In this case, the temperature, reduction strain, and reduction strain rate on hot-forging and post cooling rate are important hot-forging parameters controlling the microstructure and mechanical properties of the steels. The PHFP-M and bainitic steels [44,45] have made great achievements for weight reduction of hot-forging components in the project "Lightweight Forging Initiative" performed in Germany [1,2]. The mechanical properties and typical steel grade of the PHFP-M and bainitic steels are summarized as follows, together with Q&T steels.

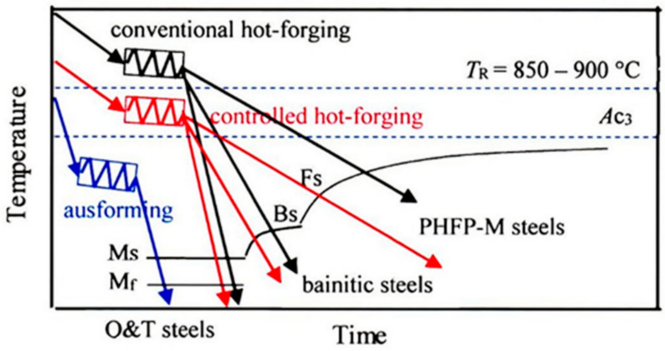

Figure 2. Conventional hot-forging, controlled hot-forging, and ausforming process followed by controlling cooling for the CFSs such as Q&T, bainitic, and PHFP-M steels. T_R: recrystallized temperature. Tempering is carried out after quenching in Q&T steel. (The figure of Ref. 46 is modified).

3.1. Q&T Steels

Conventional Q&T steels used in many hot-forged parts achieve great mechanical properties such as high yield stress, high tensile strength, large uniform and total elongations, and high impact toughness, as well as high fatigue strength, although the Q&T treatment is expensive. When the tensile strength and impact toughness are compared with those of other CFSs, Q&T steel possesses the highest tensile strength and impact toughness (Figure 3) [3,4,47]. Typical Q&T steel grade DIN-25CrMo4 and 42CrMo4 are applied to bolts and screws [4,48,49], which must be strong and tough to undergo the cyclic load. If low-cost is required for the materials, DIN-36CrB4 without Mo is replaced for the DIN-42CrMo4 [48,49], also with regard to applications such as crankshafts and shafts. Fully substituting Mo by Mn results in reduced low temperature impact toughness values [48].

Ausforming of metastable austenite is an important forging technique enhancing both the strength and impact toughness due to prior austenitic grain refining. A martensitic METT100 steel (0.07C−3.2Mn−0.6Cr−0.2Mo, in masss%) [50] has been developed by Q&T treatment after ausforming. The METT100 steel has high buckling strength two times that of DIN-S40VC (0.40C−0.2Si−1.0Mn−(0.1–0.2)V). The increased yield stress, tensile strength, and impact toughness are caused by the increased dislocation density without cell structure and refining of martensite lath and block, as well as prior austenitic grain refining [50]. The METT100 forging steel is expected to be applied to actual automotive components such as connecting rod, crank shaft, driveshaft differential, constant velocity joint, wheel carrier, suspension, etc.

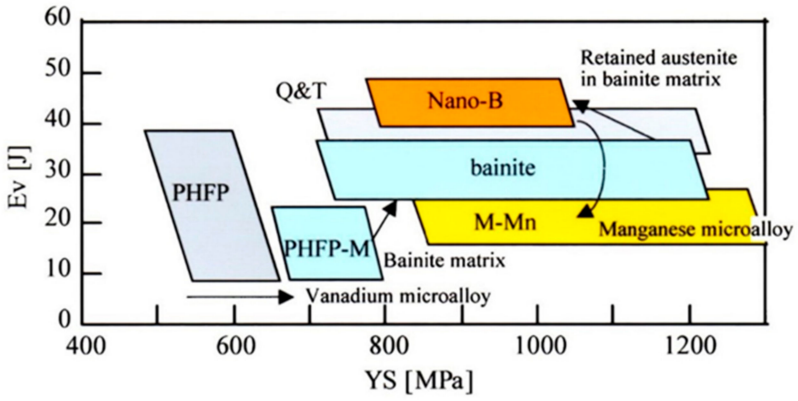

Figure 3. Relationship between Charpy V-notch impact energy (*Ev*) and yield stress (YS) at room temperature in various steel groups, mainly used for hot-forgings in the automotive industry [3,4,47]. Q&T, PHFP, PHFP-M, Nano-B, and M-Mn are quenching and tempering steel, V-microalloying precipitation-hardening ferritic-pearlitic steel, modified PHFP steel, nanostructured bainitic steel, and dual-phase type medium Mn steel, respectively.

3.2. PHFP-M Steels

PHFP-M steels developed as alternative materials of Q&T forging steels are characterized by low production cost due to the elimination of an additional Q&T step. The PHFP-M steels are achieved by reduction of the ferrite fraction, the decrease in the pearlite lamellae spacing, and the addition of the microalloying elements Nb and Ti, which results in additional precipitates besides the V(C,N) [3,38–40,45,51,52]. However, the PHFP-M steels possess lower yield strength, lower tensile strength, and lower Charpy V- notch impact energy compared to the Q&T steels, although the yield stress and tensile strength are higher than those of the PHFP steels with 0.1 to 0.4 mass% V (Figure 3). The typical steel grade is DIN-38MnVS6 [41,48] and 46MnVS5 [53] for connecting rods. The fine V,Nb,Ti-carbonitrides which were precipitated by fast cooling to about 600 °C followed by holding at the temperature [4] effectively increase the yield stress and tensile strength, with the decreased elongations and impact toughness.

Controlled hot-forging increases the yield stress and tensile strength of the PHFP-M forging steels due to the prior austenitic grain refining (and refining of ferritic and pearlitic structures), although the ferrite fraction increases [46]. In this case, forging temperatures are between 800 °C and 1000 °C. The controlled hot-forging is applied to produce METT75 steel (0.38C−0.25Si−1.0Mn−0.2Cr−0.2V) and METT80 steel (0.35C−0.25Si−1.0Mn−0.2Cr−0.3V) [54]. These steels are produced via air cooling after hot-forging, resulting in very fine VC precipitates in the ferrite phase. The non-heat-treated METT80 steel achieves high yield strength 1.6 times that of conventional S40VC steel [54]. For applications to powertrain components, ultrahigh-strength PHFP-M steel (Vanard Ultra: (0.4−0.5)C−(0.3−0.8)Si−(1−1.5)Mn−(0.15−0.25)V−(0.01−0.025)N) is also developed by Clarke et al. [55].

3.3. Bainitic Steels

Bainitic steels have an impact on the toughness−yield stress relationship intermediate between Q&T and PHFP-M steels (Figure 3) [49,56–61]. The bainitic steels with the different bainite morphologies such as acicular, upper, and lower bainites can be formed simply by controlling the post cooling rate immediately after hot-forging (Figure 2). One bainitic steel grade DIN-20MnCrMo7 is commercially available for applications to common rail and injector body [48,53,56,60]. The desired bainitic structure is achieved by adding Mn, Cr, and some Mo. Likewise, DIN-16MnCrV7-7, which is a cost-effective steel grade, achieves an attractive strength level without additional heat-treatment [48]. An important aspect of the bainitic steels is their machinability. For DIN-20MnCrMo7 with 0.15 mass% S, Biermann et al. [58] compared the machinability with that of Q&T steel DIN-42CrMo4. The bainitic steel is more difficult to machine, mainly due to its higher hardness.

Sourmail et al. [59,61] design the medium carbon bainitic forging steel grade DIN-38MnCrMoVB5 and 40MnSiCrMoB4. The benefit of the bainitic steels against Q&T steel DIN-42CrMo4 is obvious since the materials never require heat-treatment after hot-forging [48]. To further improve the mechanical properties of the bainitic steels, the development of Si bearing Nano-B steels with high ductility and high toughness continues [3,4,16,40,53,62] (Figure 3). Simultaneously, many researchers are developing dual-phase type M-Mn steels with a large amount of metastable retained austenite. Unfortunately, the toughness of the M-Mn steels is lower than bainitic steels [47,53,62] (see M-Mn steel in Figure 3). The details of the Nano-B steels are described in the following Section 4.

4. Advanced High-Strength Forging Steels; AFSs

Recently, 980−1960 MPa grade AFSs such as TBF, Nano-B, one and two-step Q&P, TBM, TM, and martensite type M-Mn forging steels with bainitic ferrite and/or martensite matrix structure have been developed for weight reduction of automotive powertrain and chassis [32–36]. These prospective AFSs contain Si and/or Al higher than 0.5 mass% to suppress the carbide formation and promote a predominant formation of carbon-enriched retained austenite [32–37]. In addition, IT process at T_{IT} higher than M_S, between M_S and M_f and lower than M_f immediately after hot-forging must be conducted to the AFSs (Figure 4). The heat-treatment of two-step Q&P steel exceptionally consists of quenching to temperature (T_Q) between M_S and M_f and subsequent partitioning at temperature (T_P) higher than M_S. In some cases, Cr, Ni, Mo, B, etc. are microalloyed to increase the hardenability of the AFSs. Further, V, Ti, and/or Nb are added to refine the prior austenitic grain. The microstructures of the AFSs are classified into three types as illustrated in Figure 5. Metastable retained austenite in all AFSs plays an important role in enhancing the ductility and fracture strengths such as fatigue strength, impact toughness, and delayed fracture strength [63,64]. In the following, the microstructural and mechanical properties of three types of AFS are detailed.

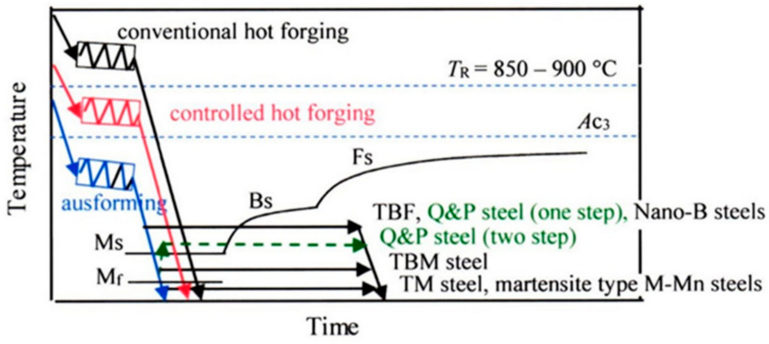

Figure 4. Hot-forging processes of low and medium carbon AFSs such as TBF, one-step and two-step Q&P, Nano-B, TBM, TM, and martensite type M-Mn steels. T_R: recrystallized temperature.

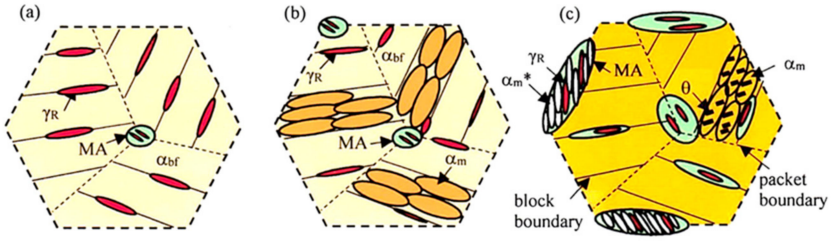

Figure 5. Illustration of typical microstructure of various AFSs. (**a**): TBF, Nano-B, and one-step Q&P steels, (**b**): two-step Q&P, TBM, and Nano-B steels, (**c**): TM and martensite type M-Mn steels. α_{bf}, α_m, α_m*, γ_R, θ, and MA represent bainitic ferrite, soft martensite, hard martensite, retained austenite, carbide, and a mixture of martensite and austenite, respectively.

4.1. TBF, One-Step Q&P, and Nano-B Steels ($T_{IT} > M_S$)

TBF steels are produced by IT process at T_{IT} higher than M_S immediately after hot-forging in austenite region, in the same way as one-step Q&P and Nano-B steels (Figure 4). The microstructure mainly consists of bainitic ferrite matrix structure, filmy retained austenite along the bainitic ferrite lath boundary, and a negligible amount of MA phase (Figure 5a).

Hot-forging with a reduction strain higher than 40% refines the prior austenitic grain, bainitic ferrite structure, retained austenite phase, and MA phase (Figure 6b) [37]. Also, the hot-forging increases the volume fraction and mechanical stability of the retained austenite. Microalloying of Cr and Mo is effective to increase the volume fraction and carbon concentration of the retained austenite, as well as an increase in hardenability [32–34]. Controlled hot-forging and ausforming followed by IT process is also further effective to refine the microstructure and improve the retained austenite characteristics [34].

Hot-forging with a reduction strain of 50% achieves an excellent combination of yield stress of 700−1000 MPa and Charpy impact absorbed value of 110–130 J/cm^2 in 0.20C−1.52Si−1.50Mn−0.05Nb−0.0018B and 0.42C−1.47Si−1.51Mn−0.50Cr−0.20Mo−0.48Al−0.05Nb TBF steels subjected to IT process at T_{IT} above M_S (Figure 7) [35,65], as well as a good balance of yield stress and total elongation. The yield stress−impact toughness balance exceeds so much that of a hot-forged 0.3C−0.26Si−1.0Mn−0.2Cr−0.3V PHFP-M steel [55] and an ausformed 0.13C−0.26Si−2.7Mn Q&T steel [50] (see Figure 7). A similar result is also obtained by El-Din et al. [66]. From the examinations of microstructure and retained austenite characteristics, it is revealed that the excellent balance of TBF steel is mainly caused by (i) refined bainitic ferrite matrix structure, (ii) refined prior austenitic grain, and (iii) a large amount of refined metastable retained austenite. The retained austenite suppresses the crack initiation or the void formation and subsequent void coalescence during impact tests via the plastic relaxation of localized stress concentration and an increase in carbon-enriched hard martensite fraction resulting from the strain-induced transformation [32,33]. Ultra-fast heating before hot-forging is also effective for grain refining [67].

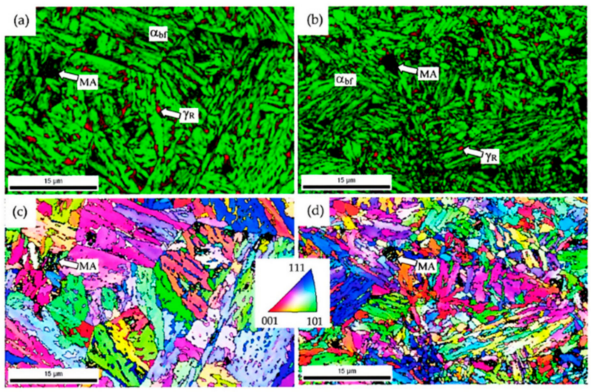

Figure 6. Phase maps (**a**,**b**) and orientation maps (**c**,**d**) of EBSP of 0.42C−1.47Si−1.51Mn−0.50Cr−0.20Mo−0.48Al−0.05Nb TBF steel subjected to IT process at T_{IT} = 350 °C immediately after (**a**,**c**) austenitizing and (**b**,**d**) hot-forging at a reduction strain of 50% and a strain rate of 0.5/s. In (**a**,**b**), α_{bf}, γ_R and MA represent bainitic ferrite (yellowish green), retained austenite (red), and martensite-austenite phase, respectively [32,33]. (**a**,**c**): $f\gamma_0$ = 20.0 vol.%, (**b**,**d**): $f\gamma_0$ = 21.2 vol.%.

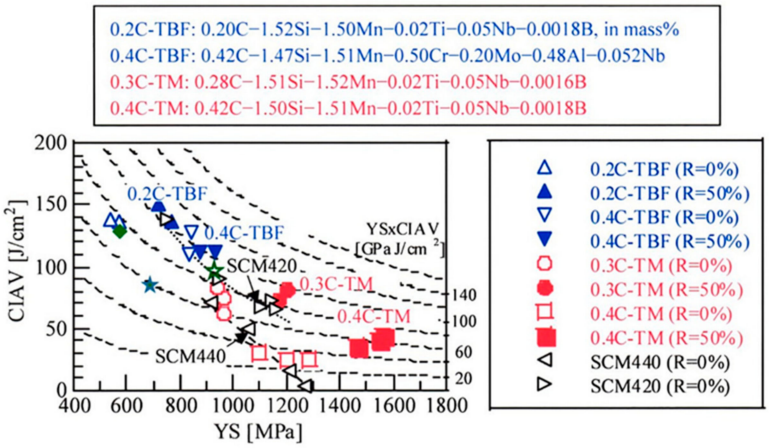

Figure 7. Charpy impact absorbed values (CIAV) as a function of yield stress or 0.2% offset proof stress (YS) in hot-forged low and medium carbon TBF and TM steels and heat-treated JIS-SCM420 and JIS-SCM440 steels [33,35,65]. Charpy impact and tensile tests were carried out at room temperature. ☆: 0.2C−1.5Si−5Mn martensite type M-Mn steel [26], ◆: 0.3C−0.26Si−1.0Mn−0.2Cr−0.3V PHFP-M steel [55], ★: 0.13C−0.26Si−2.7Mn ausformed Q&T steel [50]. *R*: reduction strain, open marks: steels without hot-forging, solid marks: steels hot-forged at a reduction strain of 50% and a strain rate of 0.5/s.

Sugimoto et al. [63,68] report that a low carbon TBF steel achieves the excellent balance of mechanical properties as shown in Figure 8. Wirths et al. [69] find out an interesting result which hot-forged 0.18C−0.97Si−2.50Mn−0.2Cr−0.1Mo−0.0018B Nano-B steel exhibits a significant cyclic hardening, differing from 42CrMo4 Q&T steel showing a large cyclic softening, in the same way as a 0.17C−1.41Si−2.02Mn TBF steel [63]. The Nano-B steel also exhibits a balance of tensile strength and Charpy impact absorbed value higher than that of Q&T steel DIN-42CrMo4. Buchmayr [4] and Caballero et al. [23] also report that low carbon Nano-B steels achieve an excellent balance of yield stress and total elongation.

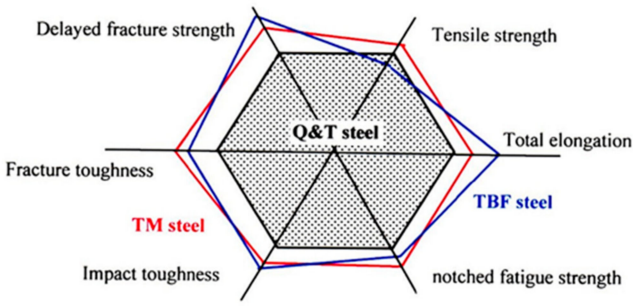

Figure 8. Comparison of various mechanical properties of DIN-22MnB5 Q&T steel and 0.2C-1.5Si-1.5Mn TBF and TM steels subjected to heat-treatment without hot-forging. This figure was modified based on Refs. [63,64].

4.2. Two-Step Q&P ($M_f < T_Q < M_S$, $T_P > M_S$) and TBM Steels ($M_f < T_{IT} < M_S$)

Two-step Q&P process consists of direct quenching to temperature (T_Q) between M_S and M_f and subsequent partitioning at temperature (T_P) higher than M_S after austenitizing [17] (green dotted line in Figure 4). On quenching, a certain amount of soft martensite transforms first. The soft martensite fraction ($f\alpha_m$) can be estimated by the following empirical equation proposed by Koistinen and Marburger [70].

$$f\alpha_m = 1 - \exp\{-A\,(M_S - T_Q)^B\} \quad (1)$$

where A and B are material constants. During partitioning, carbide-free bainite transformation results from austenite, accompanied with carbon migration from soft martensite to the remaining austenite. The resultant microstructure consists of a dual-phase structure of soft martensite and bainitic ferrite and a large amount of metastable retained austenite (Figure 5b). In some cases, a small quantity of MA phase is formed [71]. It is noteworthy that fine martensite in the MA phase is a very hard phase because it is carbon-enriched to the same extent as retained austenite. A small amount of carbide is formed only in the soft martensite lath structure when the quenching temperature is slightly higher than M_f [72]. A simplified route with direct cooling in the quenching bath for making hot-forged parts using a Q&P process is illustrated in Figure 9 [45].

The two-step Q&P process brings out a balance of tensile strength and total elongation higher than one-step Q&P process [17]. Gao et al. [73,74] report that the two-step Q&P process enhances the Charpy impact absorbed values in low carbon Si–Mn steels. According to Bagliani et al. [72] and Somani et al. [75], the two-step Q&P process lowers the ductile–brittle transition temperature of Charpy impact absorbed value in a 0.28C−1.41Si−0.67Mn−1.49Cr−0.56Mo steel and (0.19−0.22)C−(0.55−1.48)Si−(1.50−2.04)Mn−(0−1.06)Al−(0.52−1.20)Cr−(0−0.21)Mo−(0−0.79)Ni steels, respectively. Also, De Diego-Calderón et al. [76] confirm that the two-step Q&P process increases the fracture toughness of a 0.25C−1.5Si−3Mn steel.

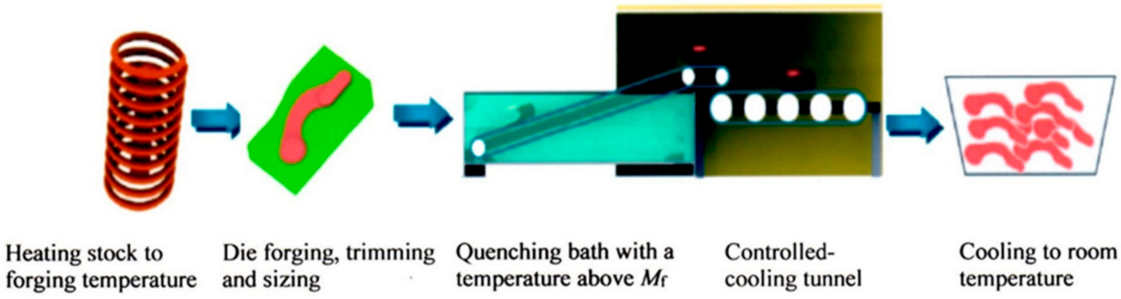

Figure 9. Simplified route with direct cooling in quenching bath for making forged parts using a two-step Q&P process (Reprinted with permission from [44], Copyright IRED 2014).

Sugimoto et al. [32,65] also reported that excellent ductility and impact toughness are obtained in hot-forged low and medium carbon TBM steels. They propose that the excellent mechanical properties are associated with (i) a refined dual-phase matrix structure of soft martensite and bainitic ferrite, (ii) refined prior austenitic grain, and (iii) a large amount of refined metastable retained austenite. The dual-phase structure plays a role in decreasing the fracture facet size and consequently lowers the ductile–brittle transition temperature. In addition, the dual-phase structure produces a compressive internal stress in the bainitic ferrite structure. A similar study using a 0.15C−1.41Si−1.88Mn−1.88Cr−0.36Ni−0.34Mo Nano-B steel subjected to ausforming and then IT process at T_{IT} between M_S and M_f is reported by Zhao et al. [77]. The roles of the above (ii) and (iii) are the same as those of TBF steels.

Although there are no data comparing the mechanical properties of hot-forged two-step Q&P steels with those of hot-forged TBM steels, the mechanical properties of the hot-forged two-step Q&P steels are supposed to be the same extent as those of the hot-forged TBM steels [64] because their microstructures are nearly the same as each other.

4.3. TM and Martensite Type M-Mn Steels ($T_{IT} < M_f$)

TM steel can be produced by IT process at T_{IT} lower than M_f immediately after hot-forging of austenite, as well as direct quenching to room temperature (Figure 4) [12–16]. If the T_{IT} is near room temperature or direct quenching to room temperature is conducted, partitioning at T_P lower than M_S is added. The microstructure is characterized by a dual-phase structure of soft martensite matrix structure and hard MA phase (Figure 5c). Most of a small amount of retained austenite is included in the MA phases [12–16]. Only a little carbide is developed only in the soft martensite, in the same way as two-step Q&P quenched to T_Q just higher than M_f and TBM steel subjected to IT process at T_{IT} just higher than M_f. Final partitioning promotes carbon-enrichment into the retained austenite and softening of both martensites without additive carbide formation [35–37].

Hot-forging at a reduction of 50% brings on an excellent combination of tensile strength of 1500 to 2000 MPa (or yield stress of 1200 to 1560 MPa) and Charpy impact absorbed value of 35 to 80 J/cm^2 in 0.3C- and 0.4C-TM steels when the partitioning process was added after the IT process (Figure 7) [35]. The combination exceeds so much those of the commercial Q&T steels such as JIS-SCM420 and SCM440 steels in a range of YS > 1200 MPa [35,65], although the combination is slightly inferior to that of TBF steels. The ductile–brittle transition temperatures, however, are much lower than those of TBF steels [64]. Also, TM steels possess higher tensile strength, delayed fracture strength, fracture toughness, and notched fatigue strength than TBF steel. As shown in Figure 7a, 0.2C–1.5Si–5Mn martensite type M-Mn steel without hot-forging exhibits the same combination of yield stress and Charpy impact absorbed value as 0.3C-TM steel, but lower combination than 0.2C- and 0.4C-TBF steels [26].

According to Kobayashi et al. [78], MA phases in the TM steel play an important role in suppressing void formation and preferential void growth at the MA phase/matrix interface (Figure 10a). Furthermore, the MA phases also inhibit the initiation and propagation of cleavage cracking (Figure 10b), through the block effect and the plastic relaxation that occurs as a result of the strain-induced transformation of the metastable retained austenite. With this is in mind, the excellent impact toughness of TM steel is mainly caused by (i) refined dual-phase structure of soft martensite and MA phase and (ii) refined prior austenitic grain [35,36]. The (i) also generates a high long range compressive internal stress in the soft martensitic matrix. A small quantity of metastable retained austenite and the decreased carbide fraction may make a contribution to the impact toughness.

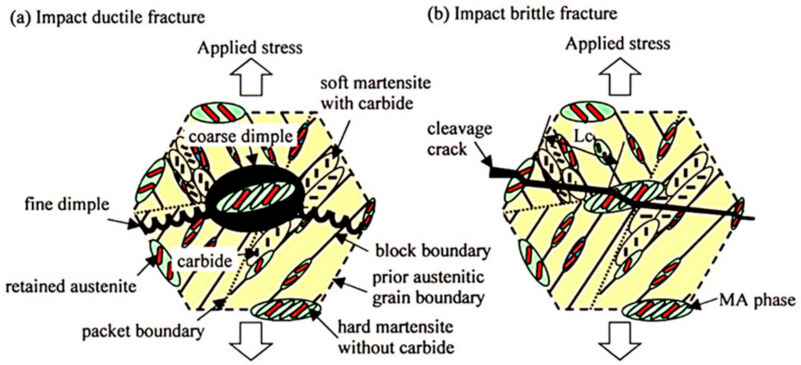

Figure 10. Illustrations showing (**a**) a ductile fracture and (**b**) a brittle fracture of TM steel appeared on impact tests [78,79]. L_c: Quasi-cleavage length affected by the MA phase located on prior austenitic, packet, and block boundaries.

5. Summary

In this paper, the hot-forging process and mechanical properties of CFSs were first stated, as well as typical steel grade and various automotive applications. Next, the microstructural and mechanical properties of HFSs were shown and compared with those of CFSs.

Hot-forged AFSs achieved much better mechanical properties than hot-forged CFSs. The excellent mechanical properties, especially impact toughness, were mainly caused by the following microstructural properties in TBF steel (and one-step Q&P and Nano-B steels), two-step Q&P steel (and TBM steel), and TM steel (and martensite type M-Mn steel).

(1) TBF, one-step Q&P, and Nano-B steels: refined bainitic ferrite matrix structure, refined prior austenitic grain, and a large amount of refined metastable retained austenite.
(2) Two-step Q&P and TBM steels: refined dual-phase structure of soft martensite and bainitic ferrite, refined prior austenitic grain, and a large amount of refined metastable retained austenite.
(3) TM and martensite type M-Mn steels: refined dual-phase structure of soft martensite and MA phase and refined prior austenitic grain.

For impact toughness, two types of dual-phase structure play roles in enhancing a compressive internal stress in soft structure and decreasing the fracture facet size. A large amount of refined metastable retained austenite suppresses the crack initiation or the void formation and subsequent void coalescence or crack growth via the plastic relaxation of localized stress concentration resulting from the strain-induced transformation of the retained austenite. The strain-induced hard martensite also plays a role in the block effect of crack growth, as well as MA phase. Although TM steel includes a small quantity of retained austenite, the metastable retained austenite makes a contribution to high impact toughness, as well as the decreased carbide.

The AFSs can be expected to enable the weight reduction and size-down of the automotive powertrain and chassis parts. In order to apply the AFSs to the automotive hot-forging components, however, other mechanical properties such as fatigue strength, delayed fracture strength, and wear properties of hot-forged AFSs must be systematically investigated in the future. In addition, it is desired that their mechanical properties are compared to those of CFSs and the other AFSs such as dual-phase type M-Mn steels [52,80,81] and TWIP steels [7–10].

To further enhance the wear resistance and fatigue strength of the AFSs, a surface layer shell hardened up to 60 HRC is needed [48,79]. Many engineers also want to know such mechanical properties of case-hardened AFSs.

Finally, authors want to emphasize that the AFSs may be applied to not only automotive powertrain and chassis parts but also the forging parts of other engineering structures such as construction machinery, airplanes, marine machinery, etc. The applications will increase many fracture strengths and resultantly bring about a great increase in reliability.

Author Contributions: The first draft of the paper has been written by K.-i.S., T.H. and A.K.S., and the final editing has been done by K.-i.S. and A.K.S.

Funding: This research received no external funding.

Acknowledgments: We thank J. Kobayashi from Ibaraki University for their kind discussion.

Conflicts of Interest: The authors declare no conflict of interest.

References

1. Raedt, H.W.; Wilke, F.; Ernst, C.S. Lightweight forging initiative—Phase II: Lightweight design potential in a light commercial vehicle. *ATZ* **2016**, *118*, 49–52. [CrossRef]
2. Raedt, H.W.; Wurm, T.; Busse, A. The lightweight forging initiative—Phase III: Lightweight forging design for hybrid cars and heavy-duty trucks. *ATZ* **2019**, *120*, 54–59. [CrossRef]
3. Keul, C.; Wirths, V.; Bleck, W. New bainitic steel for forgings. *Arch. Civ. Mech. Eng.* **2012**, *12*, 119–125. [CrossRef]
4. Buchmayr, B. Critical assessment 22: Bainitic forging steels. *Mater. Sci. Technol.* **2016**, *32*, 517–522. [CrossRef]
5. Zackay, V.F.; Parker, E.R.; Fahr, D.; Bush, R. The enhancement of ductility in high-strength steels. *Trans. Am. Soc. Met.* **1967**, *60*, 252–259.
6. De Cooman, B.C. Structure-properties relationship in TRIP steels containing carbide-free bainite. *Curr. Opinion Solid State Mater. Sci.* **2004**, *8*, 285–303. [CrossRef]
7. Bleck, W.; Guo, X.; Ma, Y. The TRIP effect and its application in cold formable sheet steels. *Steel Res. Int.* **2017**, *88*, 1700218. [CrossRef]
8. Rana, R.; Singh, S.B. *Automotive Steels—Design, Metallurgy, Processing and Applications*; Woodhead Publishing: Cambridge, UK, 2016.
9. Brux, U.; Frommeyer, G.; Grassel, O.; Meyer, L.W.; Weise, A. Development and characterization of high strength impact resistant Fe-Mn-(Al-,Si) TRIP/TWIP steels. *Steel Res. Int.* **2002**, *73*, 294–298. [CrossRef]
10. De Cooman, B.C.; Estrin, Y.; Kim, S.K. Twinning-induced plasticity (TWIP) steels. *Acta Mater.* **2018**, *142*, 283–362. [CrossRef]
11. Sugimoto, K.; Murata, M.; Song, S. Formability of Al-Nb bearing ultrahigh-strength TRIP-aided sheet steels with bainitic ferrite and/or martensite matrix. *ISIJ Int.* **2010**, *50*, 162–168. [CrossRef]
12. Sugimoto, K.; Kobayashi, J. Newly developed TRIP-aided martensitic steels. In Proceedings of the Materials Science and Technology and Exhibition 2010 (MS&T 10), Houston, TX, USA, 17–21 October 2010; pp. 1639–1649.
13. Kobayashi, J.; Pham, D.V.; Sugimoto, K. Stretch-flangeability of 1.5 GPa grade TRIP-aided martensitic cold rolled sheet steels. *Steel Res. Int. (Spec. Ed.)* **2011**, *81*, 598–603.
14. Kobayashi, J.; Song, S.; Sugimoto, K. Ultrahigh-strength TRIP-aided martensitic steels. *ISIJ Int.* **2012**, *52*, 1124–1129. [CrossRef]
15. Sugimoto, K.; Kobayashi, J.; Pham, D.V. Advanced ultrahigh-strength TRIP-aided martensitic sheet steels for automotive applications. In Proceedings of the International Symposium on New Developments in Advanced High Strength Sheet Steels (AIST 2013), Vail, CO, USA, 23–27 June 2013; pp. 175–184.
16. Pham, D.V.; Kobayashi, J.; Sugimoto, K. Effects of microalloying on stretch-flangeability of TRIP-aided martensitic sheet steel. *ISIJ Int.* **2014**, *54*, 1943–1951. [CrossRef]
17. Speer, J.G.; Edmonds, D.V.; Rizzo, F.C.; Matlock, D.K. Partitioning of carbon from supersaturated plates of ferrite with application to steel processing and fundamentals of the bainitic transformation. *Curr. Opin. Solid State Mat. Sci.* **2004**, *8*, 219–237. [CrossRef]
18. Kähkönen, J.; Pierce, D.T.; Speer, J.G.; De Moor, E.; Thomas, G.A.; Coughlin, D.; Clarke, K.; Clarke, A. Quenched and partitioned CMnSi steels containing 0.3 wt.% and 0.4 wt.% carbon. *JOM* **2016**, *68*, 210–214. [CrossRef]
19. Wang, L.; Speer, J.G. Quenching and partitioning steel heat treatment. *Metallogr. Microstruc. Anal.* **2013**, *2*, 268–281. [CrossRef]
20. Bhadeshia, H.K.D.H. Some phase transformations in steels. *Mater. Sci. Technol.* **1999**, *15*, 22–29. [CrossRef]
21. Garcia-Mateo, C.; Caballero, F.G.; Sourmail, T.; Smanio, V.; De Andres, C.G. Industrialised nanocrystalline bainitic steels—Design approach. *Int. J. Mater. Res.* **2014**, *105*, 725–734. [CrossRef]

22. Zhang, X.; Xu, G.; Wang, X.; Embury, D.; Bouaziz, O.; Purdy, G.P.; Zurob, H.S. Mechanical behavior of carbide-free medium carbon bainitic steels. *Metall. Mater. Trans. A* **2014**, *45A*, 1352–1361. [CrossRef]
23. Caballero, F.G.; Santofimia, M.J.; Garcia-Mateo, C.; Chao, J.; Garcia de Andres, C. Theoretical design and advanced microstructure in super high strength steels. *Mater. Des.* **2009**, *30*, 2077–2083. [CrossRef]
24. Cao, W.; Wang, C.; Shi, J.; Wang, M.; Hui, W.; Dong, D. Microstructure and mechanical properties of Fe–0.2C–5Mn steel processed by ART-annealing. *Mater. Sci. Eng. A* **2011**, *528*, 6661–6666. [CrossRef]
25. Seo, E.; Cho, L.; De Cooman, B.C. Application of quenching and partitioning processing to medium Mn Steel. *Metall. Mater. Trans. A* **2015**, *46A*, 27–31. [CrossRef]
26. Sugimoto, K.; Tanino, H.; Kobayashi, J. Impact toughness of medium-Mn transformation-induced plasticity-aided steels. *Steel Res. Int.* **2015**, *86*, 1151–1160. [CrossRef]
27. Raabe, D.; Ponge, D.; Dmitriva, O.; Sander, B. Nanoprecipitate-hardened 1.5 GPa steels with unexpected high ductility. *Scr. Mater.* **2009**, *60*, 1141–1144. [CrossRef]
28. Image IT Media. Nissan. Available online: http://image.itmedia.co.jp/l/im/mn/articles/1303/14/l_sp_130314nissan_03.jpg (accessed on 1 October 2019).
29. Billur, E.; Cetin, B.; Gurleyik, M. New generation advanced high strength steels: Developments, Trends and Constraints. *Int. J. Sci. Technol. Res.* **2016**, *2*, 50–62.
30. Yoshioka, N.; Tachibana, M. Weight reduction of automotive seat components using high-strength steel with high formability. *Kobe Steel Eng. Rep.* **2017**, *66*, 22–25.
31. Wang, W.; Wang, H.; Liu, S. Development of hot-rolled Q&P steel at Baosteel. In Proceedings of the 9th Pacific Rim International Conference on Advanced Materials and Processing (PRICM9), Kyoto, Japan, 1–5 August 2016.
32. Sugimoto, K.; Sato, S.; Arai, G. Hot forging of ultrahigh-strength TRIP-aided steel. *Mater. Sci. Forum* **2010**, *638–642*, 3074–3079. [CrossRef]
33. Sugimoto, K.; Sato, S.; Kobayashi, J.; Srivastava, A.K. Effects of Cr and Mo on mechanical properties of hot-forged medium carbon TRIP-aided bainitic ferrite steels. *Metals* **2019**, *9*, 1066. [CrossRef]
34. Sugimoto, K.; Itoh, M.; Hojo, T.; Hashimoto, S.; Ikeda, S.; Arai, G. Microstructure and mechanical properties of ausformed ultrahigh-strength TRIP-aided steels. *Mater. Sci. Forum* **2007**, *539–543*, 4309–4314. [CrossRef]
35. Kobayashi, J.; Sugimoto, K.; Arai, G. Effects of hot forging process on combination of strength and toughness in ultrahigh-strength TRIP-aided martensitic steels. *Adv. Mater. Res.* **2012**, *409*, 696–701. [CrossRef]
36. Kobayashi, J.; Nakajima, Y.; Sugimoto, K. Effects of cooling rate on impact toughness of an ultrahigh-strength TRIP-aided martensitic steel. *Adv. Mater. Res.* **2014**, *922*, 366–371. [CrossRef]
37. Sugimoto, K.; Kobayashi, J.; Nakajima, Y.; Kochi, T. The effects of cooling rate on retained austenite characteristics of a 0.2C-1.5Si-1.5Mn-1.0Cr-0.05Nb TRIP-aided martensitic steel. *Mater. Sci. Forum* **2014**, *783–786*, 1015–1020. [CrossRef]
38. Matlock, D.K.; Speer, J.G. Microalloying concepts and application in long products. *Mater. Sci. Technol.* **2009**, *25*, 1118–1125. [CrossRef]
39. Hui, W.; Xiao, N.; Zhao, X.; Zhang, Y.; Wu, Y. Effect of vanadium on dynamic continuous cooling transformation behavior of medium-carbon forging steels. *J. Iron Steel Res. Int.* **2017**, *24*, 641–648. [CrossRef]
40. Garcia-Mateo, C.; Morales-Rivas, L.; Caballero, F.G.; Milbourn, D.; Sourmail, T. Vanadium effect on a medium carbon forging steel. *Metals* **2016**, *6*, 130. [CrossRef]
41. Li, Y.; Milbourn, D. Vanadium microalloyed forging steel. In Proceedings of the 2nd International Symposium on Automobile Steel, Anshan, China, 21–24 May 2013; pp. 47–54.
42. Miyamoto, G.; Hori, R.; Poorganji, B.; Furuhara, T. Interface precipitation of VC and resultant hardening in V-added medium carbon steels. *ISIJ Int.* **2011**, *51*, 1733–1739. [CrossRef]
43. Hui, W.; Zhang, Y.; Shao, C.; Chen, S.; Zhao, X.; Dong, H. Enhancing the mechanical properties of vanadium-microalloyed medium-carbon steel by optimizing post-forging cooling conditions. *Mater. Manuf. Process.* **2016**, *31*, 770–775. [CrossRef]
44. Mašek, B.; Jirková, H. New material concept for forging. In Proceedings of the International Conference on Advances in Civil Structural Mechanical Engineering (ACSME 2014), Bangkok, Thailand, 4–5 January 2014; pp. 92–96.
45. Balart, M.J.; Davis, C.L.; Strangwood, M. Fracture behavior in medium-carbon Ti-V-Nb and V-Nb microalloyed ferritic-pearlitic and bainitic forging steels with enhanced machinability. *Mater. Sci. Eng. A* **2002**, *328*, 48–57. [CrossRef]

46. Fujiwara, M.; Yoshida, H.; Isogawa, S. Controlled forging technology for special steels. *Denki-Seiko* **2007**, *78*, 259–265. [CrossRef]
47. Gramlich, A.; Emmrich, R.; Bleck, W. Austenite reversion tempering-annealing of 4 wt. % manganese steels for automotive forging application. In Proceedings of the 4th International Conference on Medium and High Mn Steels, Aachen, Germany, 1–3 April 2019; pp. 283–286.
48. Raedt, H.W.; Speckenheuer, U.; Vollrath, K. New forged steels, Energy-efficient solutions for stronger parts. *ATZ* **2012**, *114*, 5–9.
49. Riedner, S.; Van Soest, F.; Kunow, S. B-alloyed quench and temper steels—An option to classic CrMo and CrNiMo quench and temper steels. In Proceedings of the 3rd International Conference on Steels for Cars and Trucks (SCT 2011), Salzburg, Austria, 5–9 June 2011; pp. 219–225.
50. Yoshida, H.; Isogawa, S.; Ishikawa, T. Basic property of martensitic microalloyed steel—Development of microalloyed steel for forging using ausforming I. *J. Jpn. Soc. Technol. Plast.* **2000**, *41*, 379–383.
51. Bleck, W.; Bambach, M.; Wirths, V.; Stieben, A. Microalloyed engineering steels with improved performance—An Overview. *Heat Treat. Mater. J.* **2017**, *72*, 355–364. [CrossRef]
52. Langeborg, R.; Sandberg, O.; Roberts, W. *Fundamentals of Microalloying Forging Steels*; Krauss, G., Banerji, S.K., Eds.; TMS: Warrendale, PA, USA, 1987; pp. 39–54.
53. Dickert, H.H.; Florian, J.C.; Gervelmeyer, J. Air-hardening high strength steels for all dimensions (of forged components). In Proceedings of the 5th International Conference on Steels for Cars and Trucks (SCT2017), Amsterdam, The Netherland, 18–22 June 2017; p. 212.
54. Yoshida, H.; Isogawa, S.; Ishikawa, T. Basic properties of ferrite-pearlitic microalloyed steel—Development of microalloyed steel for controlled forging I. *J. Jpn. Soc. Technol. Plast.* **2001**, *41*, 569–573.
55. Clarke, P.; Green, M.; Dolman, R. Development of high strength microalloyed steel for powertrain applications. In Proceedings of the 4th International Conference on Steels for Cars and Trucks (SCT2014), Braunschweig, Germany, 15–19 June 2014; pp. 442–449.
56. Engineer, S.; Justinger, H.; Janβen, O.; Härtel, M.; Hampel, C.; Randelhoff, T. Technological properties of the new high strength bainitic steel 20MnCrMo7. In Proceedings of the 3rd International Conference on Steels for Cars and Trucks (SCT 2011), Salzburg, Austria, 5–9 June 2011; pp. 404–411.
57. Gomez, G.; Pérez, T.; Bhadeshia, H.K.D.H. Air cooled bainitic steels for strong, seamless pipes Part 1—Alloy design, kinetics and microstructure. *Mater. Sci. Technol.* **2009**, *25*, 1502–1507. [CrossRef]
58. Biermann, D.; Felderhoff, F.; Engineer, S.; Justinger, H. Machinability of high-strength bainitic steel 20MnCrMo7. In Proceedings of the 3rd International Conference on Steels for Cars and Trucks (SCT 2011), Salzburg, Austria, 5–9 June 2011; pp. 471–478.
59. Sourmail, T.; Smanio, V.; Galtier, A.; Marchal, F. Bainitic steel grades for forged components: Role of transformation kinetics and design for induction hardened components. In Proceedings of the 4th International Conference on Steels for Cars and Trucks (SCT2014), Braunschweig, Germany, 15–19 June 2014; pp. 342–349.
60. Roelofs, H.; Krull, H.-G.; Lembke, M.; Lapierre Boire, L.P. Continuously cooled high strength steels: From small to large sections. In Proceedings of the 5th International Conference on Steels for Cars and Trucks (SCT2017), Amsterdam, The Netherland, 18–22 June 2017; p. 82.
61. Maminska, K.; Roth, A.; d'Eramo, E.; Marchal, F.; Galtier, A.; Sourmail, T. A new bainitic forging steel for surface induction hardened components. In Proceedings of the 5th International Conference on Steels for Cars and Trucks (SCT2017), Amsterdam, The Netherland, 18–22 June 2017; p. 228.
62. Bleck, W.; Prahl, U.; Hirt, G.; Bambach, M. Designing new forging steels by ICMPE. In *Advances in Production Technology*; Brecher, C., Ed.; Springer: Cham, Switzerland; Heidelberg, Germany, 2015; Chapter 7; pp. 85–98.
63. Sugimoto, K. Fracture strength and toughness of ultrahigh strength TRIP aided steels. *Mater. Sci. Technol.* **2009**, *25*, 1108–1117. [CrossRef]
64. Sugimoto, K.; Srivastava, A.K. Microstructure and Mechanical Properties of a TRIP-aided Martensitic Steel. *Metall. Microstr. Anal.* **2015**, *4*, 344–354. [CrossRef]
65. Sugimoto, K.; Kobayashi, J.; Arai, G. Development of low alloy TRIP-aided steel for hot-forging parts with excellent toughness. *Steel Res. Int. (Spec. Ed. Metal Form. 2010)* **2010**, *81*, 254–257.
66. El-Din, H.N.; Showaib, E.A.; Zaafarani, N.; Refaiy, H. Structure-properties relationship in TRIP type bainitic ferrite steel austempered at different temperatures. *Int. J. Mech. Mater. Eng.* **2017**, *12*, 3. [CrossRef]

67. Papaefthymiou, S.; Banis, A.; Bouzouni, M.; Petrov, R.H. Effect of ultra-fast heat treatment on the subsequent formation of mixed martensitic/bainitic microstructure with carbides in a CrMo medium carbon steel. *Metals* **2019**, *9*, 312. [CrossRef]
68. Yoshikawa, N.; Kobayashi, J.; Sugimoto, K. Notch-fatigue properties of advanced TRIP-aided bainitic ferrite steels. *Metall. Mater. Trans. A* **2012**, *43A*, 4129–4136. [CrossRef]
69. Wirths, V.; Bleck, W. Carbide free bainitic forging steels with improved fatigue properties. In Proceedings of the 4th International Conference on Steels for Cars and Trucks (SCT2014), Braunschweig, Germany, 15–19 June 2014; pp. 350–357.
70. Koistinen, D.P.; Marburger, R.E. A general equation prescribing the extent of the austenite-martensite transformation in pure iron-carbon alloys and plain carbon steels. *Acta Metal.* **1959**, *7*, 59–60. [CrossRef]
71. Kobayashi, J.; Ina, D.; Yoshikawa, N.; Sugimoto, K. Effects of the addition of Cr, Mo and Ni on the microstructure and retained austenite characteristics of 0.2%C-Si-Mn-Nb ultrahigh-strength TRIP-aided bainitic ferrite steels. *ISIJ Int.* **2012**, *52*, 1894–1901. [CrossRef]
72. Bagliani, E.P.; Santofimia, M.J.; Zhao, L.; Sietsma, J.; Anelli, E. Microstructure, tensile and toughness properties after quenching and partitioning treatments of a medium-carbon steel. *Mater. Sci. Eng. A* **2013**, *559*, 486–495. [CrossRef]
73. Gao, G.; An, B.; Zhang, H.; Guo, H.; Gui, X.; Bai, B. Concurrent enhancement of ductility and toughness in an ultrahigh strength lean alloy steel treated by bainite-based quenching-partitioning-tempering process. *Mater. Sci. Eng. A* **2017**, *702*, 104–122. [CrossRef]
74. Gao, G.; Zhang, H.; Gui, X.; Luo, P.; Tan, Z.; Bai, B. Enhanced ductility and toughness in an ultrahigh-strength Mn-Si-Cr-C steel: The great potential of ultrafine filmy retained austenite. *Acta Mater.* **2014**, *76*, 425–433. [CrossRef]
75. Somani, M.C.; Porter, D.A.; Karjalainen, L.P.; Suikkanen, P.P.; Misra, R.D.K. Process design for tough ductile martensitic steels through direct quenching and partitioning. *Mater. Today Proc.* **2015**, *2* (Suppl. 3), S631–S634. [CrossRef]
76. De Diego-Calderón, I.; Sabirov, I.; Molina-Aldareguia, J.M.; Föjer, C.; Thiessen, R. Microstructural design in quenched and partitioned (Q&P) steels to improve their fracture properties. *Mater. Sci. Eng. A* **2016**, *657*, 136–146.
77. Zhao, L.; Qian, L.; Zhou, Q.; Li, D.; Wang, T.; Jia, Z.; Zhang, F.; Meng, J. The combining effects of ausforming on the transformation kinetics, microstructure and mechanical properties of low-carbon bainitic steel. *Mater. Des.* **2019**, *183*, 108123. [CrossRef]
78. Kobayashi, J.; Ina, D.; Nakajima, Y.; Sugimoto, K. Effects of microalloying on the impact toughness of ultrahigh-strength TRIP-aided martensitic steel. *Metall. Mat. Trans. A* **2013**, *44A*, 5006–5017. [CrossRef]
79. Sugimoto, K.; Hojo, T.; Srivastava, A.K. An overview of fatigue strength of case-hardening TRIP-aided martensitic steels. *Metals* **2018**, *8*, 355. [CrossRef]
80. Tanino, H.; Horita, M.; Sugimoto, K. Impact toughness of 0.2 Pct C-1.5 Pct Si-(1.5 to 5) Pct Mn transformation-induced plasticity-aided steels with an annealed martensite matrix. *Metall. Mater. Trans. A* **2016**, *47A*, 2073–2080. [CrossRef]
81. Gramlich, A.; Emmrich, R.; Bleck, W. Austenite reversion tempering-annealing of 4 wt.% manganese steels for automotive forging application. *Metals* **2019**, *9*, 575. [CrossRef]

© 2019 by the authors. Licensee MDPI, Basel, Switzerland. This article is an open access article distributed under the terms and conditions of the Creative Commons Attribution (CC BY) license (http://creativecommons.org/licenses/by/4.0/).